Enhancement and Control of H_2 Dissociative Ionization by Femtosecond VUV Laser Pulses

A. Palacios,[1] H. Bachau,[2] and F. Martín[1]

[1]*Departamento de Química, C-9, Universidad Autónoma de Madrid, 28049 Madrid, Spain*
[2]*Centre des Lasers Intenses et Applications (UMR 5107 du CNRS-CEA-Université de Bordeaux I), 351 Cours de la Libération, F-33405 Talence, France*

(Received 17 November 2005; published 10 April 2006)

We report *ab initio* calculations of H_2 ionization by VUV/fs 10^{12} W/cm^2 laser pulses including correlation and all electronic and vibrational degrees of freedom (DOF). Inclusion of the nuclear DOF leads to a substantial increase of resonance enhanced multiphoton ionization. By varying pulse duration, it is possible to control the ratio of dissociative to nondissociative ionization as well as the final H_2^+ vibrational distribution. For pulses longer than 10 fs and $\hbar\omega > 0.46$ a.u., dissociative ionization entirely dominates, which is a very unusual situation in photoionization studies.

DOI: 10.1103/PhysRevLett.96.143001 PACS numbers: 33.80.Rv

The production of femto (fs) and subfemtosecond (sub-fs), VUV and XUV laser pulses by means of high-order harmonic generation [1–3] or free electron lasers [4–6] has opened up the way to investigate elementary two- and three-photon ionization processes in simple atoms (He, Ne, ...) [3,7,8] and molecules (H_2^+, H_2, ...) that can be accurately described by theory. Such pulses are ideal to investigate physical problems at the atomic and molecular time scales. Indeed, the dynamics of bound electronic states typically occurs in the sub-fs time scale (the revolution time of an electron orbiting around a proton is ~150 asec) and that of autoionizing states, although generally much slower, occurs in the fs time scale. Recent experiments on rare gas atoms have taken advantage of this fact to provide interesting temporal pictures of ionization [2,9,10] and autoionization [10].

Molecular processes are even more interesting due to the presence of the nuclear motion, which manifests through rotation, vibration, and the possibility of dissociation [11]. Vibration and rotation typically occur in the fs time scale and, therefore, may compete efficiently with slow electronic processes such as autoionization [12,13]. Thus the use of VUV and XUV/fs pulses allows one to explore the possibility of controlling molecular dissociation and ionization. Nevertheless, realistic theoretical investigations on molecular systems are very scarce, mainly due to the complexity in accounting for both the electronic and nuclear degrees of freedom (DOF). Most theoretical applications have focused on the simplest H_2^+ molecule and have made use of the fixed nuclei approximation (FNA) [14–17]. The FNA is useful when the electron response is much faster than the typical vibrational period of the molecule. This is not the case when ionization is mediated by electronic resonances, because the nuclei have the time to move before the electrons are ejected. Resonant dissociative ionization of H_2^+ including the nuclear DOF has been studied by means of low dimensional models [18–20] (IR/fs pulses) and, very recently, full dimensional theories [21,22] (XUV/fs pulses).

H_2 is much easier to handle experimentally than H_2^+ and, therefore, it is more convenient for direct comparisons with theory. However, theoretical calculations including all DOF are even scarcer than for H_2^+. This is due to the additional difficulty introduced by electron correlation. In early works, this was overcome by using the single-active electron approximation. Only recently, fully correlated calculations have become accessible, but always within the FNA [23–25]. In this work we present *ab initio* theoretical calculations of H_2 dissociative (DI) and nondissociative ionization (NDI) induced by VUV/fs laser pulses by including all electronic and vibrational DOF, as well as electron correlation. A typical laser intensity of 10^{12} W/cm^2 has been chosen. We show that inclusion of the nuclear DOF leads to a dramatic increase of resonance enhanced multiphoton ionization (REMPI) and that, by increasing the pulse duration, DI becomes the dominant process. This is an unexpected result because, in all reported studies on H_2 photoionization, DI is always orders of magnitude smaller than NDI.

Figure 1 shows the relevant potential energy curves of H_2 as well as the typical two- and three-photon ionization processes. We consider ionization of H_2 from the $X^1\Sigma_g^+$ ground state using linearly polarized light. We restrict our study to the dipole approximation and to the case of H_2 molecules oriented along the polarization direction of the incident light. In this particular case, the dipole selection rule imposes that the first absorbed photon couples the initial $X^1\Sigma_g^+$ state to states of $^1\Sigma_u^+$ symmetry, the second photon couples the latter to states of $^1\Sigma_g^+$ symmetry, and so on. Only bound and continuum electronic states of these two symmetries are shown in Fig. 1. We have solved the time-dependent Schrödinger equation

$$i\frac{\partial}{\partial t}\Phi(\mathbf{r}, R, t) = [H + V(t)]\Phi(\mathbf{r}, R, t), \qquad (1)$$

where H is the Hamiltonian of H_2 in the body-fixed frame and $V(t) = \mathbf{p}\cdot\mathbf{A}(t)$ is the laser-molecule interaction po-

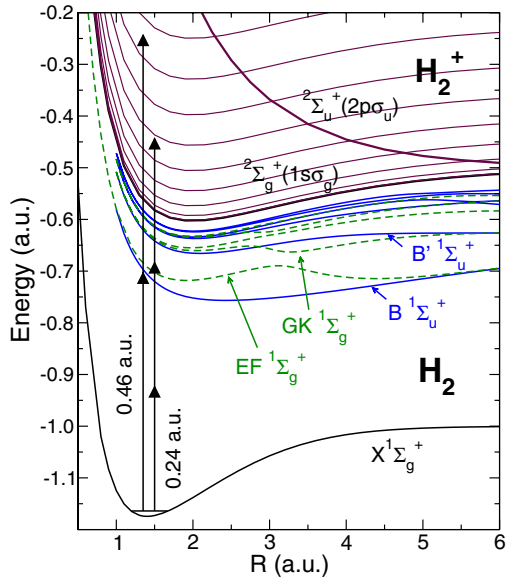

FIG. 1 (color online). Potential energy curves of H_2 as functions of internuclear distance. The figure shows the six lowest states of $^1\Sigma_g^+$ and $^1\Sigma_u^+$ symmetries, the $^2\Sigma_g^+(1s\sigma_g)$ and $^2\Sigma_u^+(2p\sigma_u)$ ionization thresholds, and a typical discretized electronic continuum. The typical two- and three-photon transition leading to ionization are indicated by arrows (the corresponding photon energies are also given).

tential in the velocity gauge. The vector $\mathbf{r}$ indicates all electronic coordinates and R is the internuclear distance. For a photon energy ω and a pulse duration T, the vector potential $\mathbf{A}(t)$, polarized along the vector $\mathbf{e}_z$ (the direction of the internuclear axis), is defined as

$$\mathbf{A}(t) = \begin{cases} A_0 f(t)\cos(\omega t + \phi)\mathbf{e}_z; & t \in [-T/2, +T/2] \\ 0; & \text{elsewhere.} \end{cases} \tag{2}$$

where $f(t)$ is the pulse envelope and ϕ is the pulse phase. All results in this work have been obtained for a cosine envelope, $f(t) = \cos^2(\pi t/T)$, and $\phi = 0$. In a few cases, that will be explicitly indicated, we have also considered Gaussian envelopes and different phases.

To solve Eq. (1), we have extended the methods used in our previous study of H_2^+ ionization [21,22,26]. Briefly, the time-dependent molecular wave function $\Phi(\mathbf{r}, R, t)$ is expanded in a basis of stationary vibronic states $\Psi_{n\nu_n}(\mathbf{r}, R)$. Neglecting rotational effects, these states are written, in the Born-Oppenheimer approximation,

$$\Psi_{n\nu_n}(\mathbf{r}, R) = R^{-1}\chi_{\nu_n}(R)\psi_n(\mathbf{r}, R), \tag{3}$$

where ψ_n and χ_{ν_n} are the usual electronic and vibrational wave functions. From the expansion coefficients, $c^{(l)}_{n\nu_n}(t)$, the ionization probability, differential in the H_2^+ energy $W_{n\nu_n}$, is given by the integral over the ejected electron energy [22]

$$\frac{dP}{dW_{n\nu_n}} = \sum_l \int d\varepsilon_n |c^{(l)}_{n\nu_n}(t = T/2)|^2. \tag{4}$$

For DI, $W_{n\nu_n}$ is directly related to the center-of-mass (c.m.) energy of the outgoing protons, $E_{H^+} = W_{n\nu_n} - E_\infty$, where E_∞ is the energy of a H atom infinitely separated from H^+. For NDI, $W_{n\nu_n}$ is the vibronic energy of the residual H_2^+ ion. Integrating (4) over $W_{n\nu_n}$ gives the total ionization probability P.

Electronic bound states of H_2 have been evaluated by expanding the electronic wave functions ψ_n in a basis of configurations built from H_2^+ orbitals and Slater-type orbitals. All these orbitals have been represented through a one-center expansion that includes spherical harmonics up to $l = 16$. The corresponding radial parts have been expanded in a basis of 180 B splines of order $k = 8$ in a box of radial length of 60 a.u. (see [27] for details). Our calculated energies and dipole couplings are in good agreement with those reported by Wolniewicz *et al.* (see [28,29] and references therein). Figure 1 shows the six lowest states of $^1\Sigma_g^+$ and $^1\Sigma_u^+$ symmetries.

For a given value of R, the electronic continuum states of energy $\varepsilon_n(R)$ must satisfy the usual boundary conditions corresponding to one electron in a bound electronic state of H_2^+ and the other electron in a single outgoing spherical wave with a well-defined value of the angular momentum l and a combination of incoming spherical waves for all possible values of the angular momentum compatible with the molecular symmetry [30]. For a given $\varepsilon_n(R)$ energy, there exists a continuum state for each outgoing l [this is the reason why the index l is included in $c^{(l)}_{n\nu_n}(t)$]. These states have been evaluated by means of the L^2 close-coupling method (see [30] and references therein) by using the same H_2^+ orbitals and B-spline functions as for bound states. In this case, we have found that convergence is practically achieved by including partial waves for the ejected electron up to $l = 3$. Vibrational (bound and dissociative) wave functions have been expanded in a basis of 240 B splines of order $k = 8$ contained in a box of 12 a.u. The size of the electronic (nuclear) box has been chosen so that $\Delta\varepsilon_n(\Delta W_{n\nu_n}) \ll \Delta\omega$, where $\Delta\omega$ is the laser bandwidth. This condition ensures that the electronic (vibrational) wave packet does not reach the limit of the electronic (vibrational) box before the end of the pulse. As illustration, a typical discretized electronic continuum is shown in Fig. 1.

In the expansion of $\Phi(\mathbf{r}, R, t)$, we have included all vibronic states with total energy ≤ 0 a.u. corresponding to the six lowest $^1\Sigma_g^+$ states, the six lowest $^1\Sigma_u^+$ states, and all discretized electronic continuum states of both symmetries that are compatible with that condition and leave the residual electron in the $1s\sigma_g$ orbital. With this basis set, we have obtained two- and three-photon ionization cross sections within the FNA that are practically identical to those obtained by Awasthi *et al.* [25].

Figure 2 shows the calculated ionization probabilities as functions of photon energy for pulses of 10 and 2 fs. For the longer pulse, a significant enhancement of the total ionization probability is observed at the N-photon ionization thresholds. This is in agreement with the FNA results. These thresholds are barely visible for the shorter pulse, which is the consequence of the larger bandwidth. For $\omega > 0.35$ a.u., where two-photon ionization dominates, inclusion of the nuclear motion leads to probabilities that are much larger than the FNA ones. This is precisely the region where (1 + 1) REMPI through the $B^1\Sigma_u^+$ state occurs (see Fig. 1). The oscillation of the REMPI structure found in the FNA disappears when the nuclear motion is accounted for. The enhancement of the (1 + 1) REMPI structure is due to the favorable Franck-Condon (FC) overlap between the initial vibrational state and those of the $B^1\Sigma_u^+$ intermediate state. In contrast, no enhancement with respect to the FNA results is found for (2 + 1) REMPI ($\omega \sim 0.24$ a.u.) due to the less favorable FC overlaps with the double-well $^1\Sigma_g^+$ intermediate states (see Fig. 1). This shows the important role of electron correlation in (2 + 1) REMPI, since double wells result from the interaction between singly and doubly excited electronic configurations [28].

Another interesting conclusion is that, in the 10 fs case, DI becomes very important and even dominant in the two-photon REMPI region ($\omega > 0.35$ a.u.). This is a very striking phenomenon because, for neutral molecules, DI is usually orders of magnitude smaller than NDI. This unexpected finding results from the combination of efficient FC factors between the ground $X^1\Sigma_g^+(v = 0)$ and the $^1\Sigma_u^+(v)$ intermediate states, and between the latter and the dissociative states of the $^1\Sigma_g^+$ electronic states. Such a vibrational selectivity can only be achieved for pulses with a narrow bandwidth, i.e., typically of the order of the vibrational energy spacing of the states involved. This explains why, as shown in Fig. 2(b), DI is no longer dominant for the 2 fs pulse. A similar loss of vibrational selectivity is responsible for the dominant role of NDI when more than two photons are absorbed.

The above reasonings suggest that the relative importance of DI vs NDI can be controlled by varying the pulse duration. This is illustrated in Fig. 3 where the variation of the dissociative and nondissociative probabilities with pulse duration is shown for a fixed photon energy of 0.49 a.u.. It can be seen that both probabilities vary with pulse duration in a monotonous way and that the DI probability increases by more than 2 orders of magnitude when the pulse duration is varied from 2 to 12 fs. As Fig. 3 shows, the results are practically the same for different pulse envelopes and phases, which is not surprising because all pulses considered in this work contain a large number of cycles.

Figure 4 shows the vibrational distribution of H_2^+ ions and the proton kinetic energy distribution (KED) for three pulse durations and a photon energy that leads to maximum

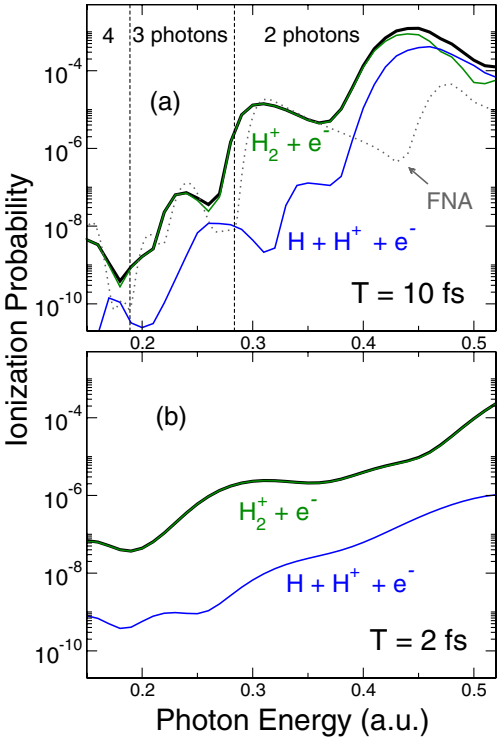

FIG. 2 (color online). Total (thick line) and partial (thin lines) ionization probabilities vs photon energy for $I = 10^{12}$ W cm^{-2} and (a) $T = 10$ fs and (b) $T = 2$ fs. Dotted line: results of the FNA. Vertical dashed lines indicate the positions of the N-photon ionization thresholds.

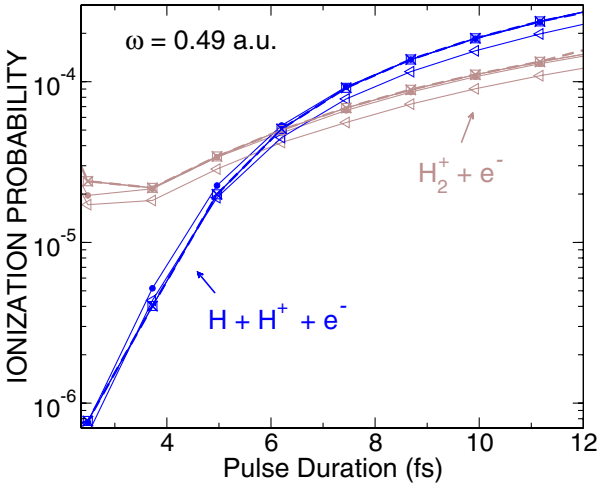

FIG. 3 (color online). Variation of dissociative and nondissociative ionization probabilities with pulse duration at a fixed photon energy $\omega = 0.49$ a.u. and intensity $I = 10^{12}$ W cm^{-2}. Full lines: cosine envelope; circles: Gaussian envelope with the same full width at half maximum (FWHM); triangles: Gaussian envelope with the same integral. All previous results obtained with $\phi = 0$. Squares: cosine envelope and $\phi = \pi$; crosses: cosine envelope and $\phi = \pi/2$.

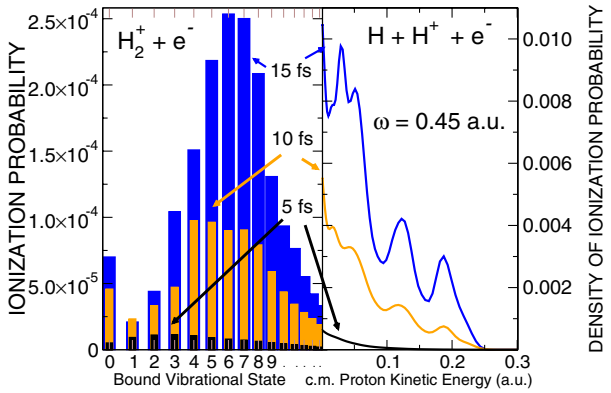

FIG. 4 (color online). Vibrational distribution of H_2^+ ions (left) and proton kinetic energy distribution (right) for different pulse durations, $\omega = 0.45$ a.u. and $I = 10^{12}$ W cm^{-2}.

REMPI. For the shortest pulses (≤ 5 fs), the probability distribution follows a typical one-photon FC behavior: H_2^+ is mainly produced in a vibrational state around $v = 2$ and the H^+ KED decays exponentially. This is similar to what has been found for H_2^+ [22] and is the consequence of the large bandwidth that dilutes resonant transitions. However, Fig. 4 shows that, for the longer pulses, the calculated probability does not follow this simple FC behavior. As the pulse duration increases, H_2^+ is left in higher and higher vibrational states and the H^+ KED exhibits more and more pronounced oscillations. This is because the FC overlaps associated with the second photon transition oscillate with energy: when the nodes in the final vibrational state coincide with the nodes in the intermediate vibrational state, a maximum overlap is obtained; when maxima coincide with nodes, a minimum overlap is obtained. For photon energies outside the REMPI regions, we have always found probability distributions that follow a FC behavior, both for short and long pulses.

In conclusion, inclusion of the nuclear degrees of freedom in the description of H_2 ionization by VUV/fs laser pulses has a dramatic effect in REMPI: the latter can be several orders of magnitude larger than predicted by the fixed nuclei approximation. Furthermore, by varying the pulse duration, it is possible to control the DI/NDI ratio as well as the final vibrational distribution of the ionized molecule. For pulses with $\omega > 0.46$ a.u. and $T > 10$ fs, dissociative ionization entirely dominates, which is a very unusual situation in photoionization studies.

Work supported by the DGI (Spain) Project No. BFM2003-00194 and the European COST action D26/0002/02. We thank the CCC-UAM (Madrid, Spain) for computer time.

[1] P. Agostini and L. F. DiMauro, Rep. Prog. Phys. **67**, 813 (2004).
[2] R. Kienberger *et al.*, Nature (London) **427**, 817 (2004).
[3] H. Mashiko, A. Suda, and K. Midorikawa, Opt. Lett. **29**, 1927 (2004).
[4] J. Andruszkow *et al.*, Phys. Rev. Lett. **85**, 3825 (2000).
[5] H. Wabnitz *et al.*, Nature (London) **420**, 482 (2002).
[6] V. Ayvazyan *et al.*, Phys. Rev. Lett. **88**, 104802 (2002).
[7] N. Miyamoto, M. Kamei, D. Yoshitomi, T. Kanai, T. Sekikawa, T. Nakajima, and S. Watanabe, Phys. Rev. Lett. **93**, 083903 (2004).
[8] Y. Nabekawa, H. Hasegawa, E. J. Takahashi, and K. Midorikawa, Phys. Rev. Lett. **94**, 043001 (2005).
[9] E. Goulielmakis *et al.*, Science **305**, 1267 (2004).
[10] M. Drescher, M. Hentschel, R. Kienberger, M. Uiberacker, V. Yakovlev, A. Scrinzi, T. Westerwalbesloh, U. Kleineberg, U. Heinzmann, and F. Krausz, Nature (London) **419**, 803 (2002).
[11] A. Apalategui, A. Saenz, and P. Lambropoulos, Phys. Rev. Lett. **86**, 5454 (2001).
[12] I. Sánchez and F. Martín, Phys. Rev. Lett. **79**, 1654 (1997).
[13] I. Sánchez and F. Martín, Phys. Rev. Lett. **82**, 3775 (1999).
[14] D. Dundas, J. F. McCann, J. Parker, and K. T. Taylor, J. Phys. B **33**, 3261 (2000).
[15] J. Colgan, M. S. Pindzola, and F. Robicheaux, Phys. Rev. A **68**, 063413 (2003).
[16] S. Barmaki, S. Laulan, H. Bachau, and M. Ghalim, J. Phys. B **36**, 817 (2003).
[17] A. D. Bandrauk, S. Chelkowski, and I. Kawata, Phys. Rev. A **67**, 013407 (2003).
[18] T. D. G. Walsh, F. A. Ilkov, S. L. Chin, F. Chateauneuf, T. T. Nguyen-Dang, S. Chelkowski, A. D. Bandrauk, and O. Atabek, Phys. Rev. A **58**, 3922 (1998).
[19] T. Zuo and A. D. Bandrauk, Phys. Rev. A **52**, R2511 (1995).
[20] T. Seideman, M. Y. Ivanov, and P. B. Corkum, Phys. Rev. Lett. **75**, 2819 (1995).
[21] A. Palacios, H. Bachau, and F. Martín, J. Phys. B **38**, L99 (2005).
[22] A. Palacios, S. Barmaki, H. Bachau, and F. Martín, Phys. Rev. A **71**, 063405 (2005).
[23] J. Colgan, D. Glass, K. Higgins, and P. Burke, J. Phys. B **34**, 2089 (2001).
[24] A. Apalategui and A. Saenz, J. Phys. B **35**, 1909 (2002).
[25] A. Awasthi, Y. V. Vanne, and A. Saenz, J. Phys. B **38**, 3973 (2005).
[26] S. Barmaki, H. Bachau, and M. Ghalim, Phys. Rev. A **69**, 043403 (2004).
[27] H. Bachau, E. Cormier, P. Decleva, J. E. Hansen, and F. Martín, Rep. Prog. Phys. **64**, 1815 (2001).
[28] A. de Lange, W. Hogervost, W. Ubachs, and L. Wolniewicz, Phys. Rev. Lett. **86**, 2988 (2001).
[29] L. Wolniewicz and G. Staszewska, J. Mol. Spectrosc. **217**, 181 (2003).
[30] F. Martín, J. Phys. B **32**, R197 (1999).